International Journal of NanoScience and Nanotechnology.
ISSN 0974-3081 Volume 4, Number 3 (2013), pp. 223-232
© International Research Publication House
http://www.irphouse.com

Transport Studies on Substitutional Effect in Chemically Grown Nanostructured Manganite Films

N.A. Shah

Department of Electronics,
Saurashtra University, Rajkot 360 005, India
E-mail: snikesh@yahoo.com

Abstract:

In this communication, the thin films of $La_{0.8-x}Pr_{0.2}Sr_xMnO_3$ (LPSMO) (x = 0.1, 0.2 & 03) manganites, having thickness ~ 50nm, have been chemically grown on single crystalline *(100)* $LaAlO_3$ (LAO) substrate using low cost sol-gel method. X-ray diffraction (XRD) and atomic force microscopy (AFM) have been carried out on all the films for their structural and microstructural studies, respectively, which suggest that, all the films possess nano sized crystals with the crystallite size (CS) varying between ~ 16nm and ~ 31nm while microstrain decreases from –4.23% to –2.01% with increase in CS. Transport studies using resistivity measurements reveal the decrease in resistivity and increase in metal – insulator transition temperature (T_P) with strain, CS, surface roughness (SR) and substitution (x). Variation in magnetoresistance (MR) with temperature under low field (0.7T) suggests the strong intrinsic component contribution to the magnetotransport properties of the films. Effect of substitution (x) on the transport, MR and temperature sensitivity has been discussed in the context of structural parameters and grain morphology of the films.

Key Words: Transport, Substitutional Effect, Chemical Synthesis, Nanostructure, Manganite, Thin Film

Introduction

Historically, mixed valent perovskite manganites were studied in the fifties, both, experimentally and theoretically. The experiments performed on manganites showed antiferromagnetic (AF) insulating behavior at low and high x values in $R_{1-x}A_xMnO_3$ (RE = rate earth, M = Ca, Sr, Ba, Pb) and show ferromagnetic – paramagnetic transition (T_C) followed by metal – insulator transition (T_P) in a certain range of

concentrations centered on x = 1/3 [1 – 3]. This striking behavior was early explained by the theory of double exchange (DE) [4]. Then after, it is observed that, only DE cannot explain the complete physical picture of manganites, and hence, one more aspect of the manganites, has been added, i.e. Jahn-Teller effect [5]. Emergence of intense interest was primarily stimulated by the discovery of the colossal magnetoresistance (CMR) effect in thin films of manganese oxides. CMR materials exhibit large changes in electrical resistance when an external magnetic field is applied. The magnetoresistance is defined as, MR% = $[\Delta\rho/\rho(0)] = [\{\rho(H) - \rho(0)\}/\rho(0)] \times 100$, where $\rho(H)$ and $\rho(0)$ are the resistivities at a given temperature in the presence and absence of a magnetic field (H), respectively. Mixed valent manganites are expected to exhibit MR effect as high as ~ 100%. The physical properties of manganites are determined by three main parameters: (i) substitution level (x) = Mn^{4+} / (Mn^{3+} + Mn^{4+}), (ii) average size of the cation A, $\langle r_A \rangle$ and (iii) degree of disorder at A-site, defined by $\sigma^2 = r^2_A - \langle r_A \rangle^2$, which affect the transport of manganites [6 – 8].

Manganites have been studied in polycrystalline bulk [9], thin film [10], device [11], nanostructured multilayer [12], heterostructure [13], nanostructured film [14] and nanostructured bulk [15] forms for their attracting transport properties as well as possible spintronic applications. Kuberkar et al have reported the simultaneous effect of size disorder as well as particle / grain size on the transport and magnetotransport properties of nanostructured manganites [16]. They have explained the size and disorder dependent variation in the transport in the context of nature of the particle surface and grain boundaries. Most of the reports suggest that, with increase in particle / grain size, resistivity gets reduced while T_P increases in nanostructured manganites which have been discussed in the light of grain boundary density and nature [17, 18]. Although, opposite behavior in the variation in resistivity, T_P and MR with grain size has also been reported for nanostructured $La_{0.7}Pb_{0.3}MnO_3$ manganites by Solanki et al, which has been discussed in detail on the basis of anomalous grain formation and effect of ordered grain boundaries [19]. They have separated out two contributions of MR, on the basis of the origin of MR, such as low temperature low field MR (extrinsic MR) and high field MR at ~ T_P (intrinsic MR). Parmar et al have studied the effect of annealing time and temperature on the structure and morphology and how structural and microstructural parameters govern the transport and magnetotransport behavior of nanostructured $La_{0.7}Sr_{0.3}MnO_3$ manganite films grown using chemical solution deposition (CSD) technique [14].

By keeping in mind what we have discussed, in this communication, the substitutional effects have been discussed in the light of size disorder, crystallite size, microstrain and grain morphology in nanostructured $La_{0.8-x}Pr_{0.2}Sr_xMnO_3$ (LPSMO) (x = 0.1, 0.2 & 03) manganite films grown on $LaAlO_3$ (LAO) substrates using low cost sol-gel technique.

Experimental Details

Nanostructured $La_{0.8-x}Pr_{0.2}Sr_xMnO_3$ (LPSMO) (x = 0.1, 0.2 & 03) manganite solution was chemically synthesized using sol-gel method followed by thin film fabrication,

with desired thickness ~ 50nm, on single crystalline *(100)* $LaAlO_3$ (LAO) substrates using spin-coater deposition technique. La, Pr, Sr and Mn – acetates were taken as starting materials, dissolved them into double distilled water and acetic acid (1:1 ratio) and mix, stir and heat the solution at 80°C for 30 min. Drop of a clear solution was coated on LAO substrate and spin the films at 5000 rpm for 30 sec to achieve desired thickness ~ 50nm. The films were calcined at 350°C for 30 min and then annealed them at 900°C for 6 hrs in O_2 environment. Hereafter, films substituted with 10, 20 & 30% Sr^{2+} are referred as S1, S2 and S3, respectively. All the films were characterized for their structural and microstructural properties using XRD and AFM, respectively. Temperature dependent resistance has been carried out under 0 and 0.7T applied magnetic fields.

Results and Discussion

Figure 1 shows the XRD patterns of all the three nanostructured LPSMO films. Inset shows an enlarged view of *(200)* peaks of film and substrate. The following observations can be noted from the structural analysis of the films –

i. As shown in the inset of figure 1, the intensity increases, from S1 to S3, indicating the increase in crystallinity of the films.

ii. Separation between peaks of film and substrate increases with x while the peak position shifts towards higher 2θ value suggesting the decrease in lattice parameters with x.

iii. Presence of splitting in the XRD peaks of film and substrate indicates the presence of strain at the film – substrate interface, which can be calculated using the formula:

$$\delta(\%) = [(d_{substrate} - d_{film}) / d_{substrate}] \times 100$$

In the present case, $d_{substrate} > d_{film}$ and also with increase in Sr^{2+} substitution (x), from S1 to S3, spacing d decreases and hence the strain (δ) decreases. The signature of δ is negative indicating the nature of strain is compressive type in nature. The decrease in strain can be correlated with the improved structural quality due to enhanced larger Sr^{2+} content (x) from S1 to S3 which improves the structure by modifying the Mn – O – Mn bond angles.

iv. Values of calculated crystallite size (CS) are highlighted in the figure 1. CS can be calculated using the formula:

$$CS = 0.9\lambda / B\cos\theta$$

It is clear that, with increase in x, CS increases, which supports the observation of improved crystallinity of the films with x. The size of the crystals (CS) is in the range of 16mn – 31nm confirming the nanostructured nature of the thin films.

In order to understand the nature of grains, grain boundaries, complete picture of grain morphology and to estimate (roughly) the thickness of the films, AFM has been performed on all the films. AFM micrographs of all the three films are shown in figure 2. Left panel of figure shows the AFM pictures of films while right panel

shows the granular height profile of the films. Following observation can be drown from the AFM measurements –

i. Grain size increases from 15 (± 5) nm (S1) to 35 (± 5) nm (S2) and 60 (± 10) nm (S3) with increase in x. The grain boundary density decreases while compactness of the grains increases with increase in x.
ii. The nature of the grain boundaries gets improved, i.e. width decreases while sharpness and clarity increase, with increase in x.
iii. It is clearly seen from the right panel of the figure 2 that, the maximum grain height increases from S1 (30nm) to S2 (35nm) and S3 (~ 50nm), suggesting the maximum observed film thickness is ~ 50nm.
iv. The ratio of the values of grain size to film thickness, ~ 0.5, 1.0 and 1.2 respectively for S1, S2 and S3 films which confirms the decrease in surface roughness, 19.02nm (S1), 13,43nm (S2) and 13.35nm (S3), observed from the AFM results analysis.
v. Overall, with increase in x, the increased grain size, improved grain boundary nature, enhanced grain size / film thickness ratio and decreased roughness of the film surface indicate the improved granular morphology of the films.

It is also clear from the valance balance calculations that, with increase in x from 0.1 to 0.3, the generated Mn^{4+} (expected, if the films are stoichiometrically perfect) are 10, 20 and 30%, respectively, which results into the enhanced zener double exchange mechanism and hence the transport gets enhanced in the films with x. In order to understand the resistivity behavior of the films and to correlate the transport results with the structure, microstructure and improved zener double exchange mechanism (Mn^{4+} ion density), temperature dependent resistivity has been carried out on all the three films in the temperature range ~ 100 to 200K under 0 and 0.7T applied magnetic fields. ρ – T plots of LPSMO films are shown in figure 3. The following observations are noted from figure 3 –

i. Resistivity decreases from S1 to S3 with increase in x while metal – insulator transition (T_P) increases with x, 221K (S1), 333K (S2) and 365K (S3), indicating the improved transport in presently studied nanostructured manganite films.
ii. Below 200K, difference between the ρ – T plots carried out under 0 and 0.7T fields, decreases with increase in x suggesting the low temperature spin polarization of the films which gets improved with increase in x.
iii. Applied magnetic field can suppress the resistivity, throughout the temperature range studied, indicates the exhibition of negative MR by all the films studied.

The observations of the transport measurements can be understood as follows –

i. In the present case of Sr^{2+} substituted nanostructured 50nm films, average ionic radius increases from 1.218 Å (S1) to 1.237 Å (S3) as well as tolerance factor increases from 0.833 (S1) to 0.939 (S3) which directly supports the transfer integral of charge carriers, e_g electrons, in LPSMO

system, by improving the Mn – O bond lengths and Mn – O – Mn bond angles [6].

ii. The decrease in resistivity with x can be attributed to the improved crystalline nature of the films as well as increased value of CS. Also, the Mn – O – Mn bond angles are modified resulting into the enhanced charge transfer integral and hence reduction in resistivity with x [15].

iii. Grain size increases while grain boundary density decreases with x. Also, the nature of the grain boundaries gets improved which results into the decrease in charge carrier scattering at the grain boundaries and at the Mn – O – Mn bond angles which results into the suppression in the resistivity [10].

iv. Decrease in interface strain and surface roughness of the films with x supports the transport of the films and hence resistivity decreases [20].

v. Increase in T_P with x from 221K (S1) to 365K (S3) can be ascribed to the enhanced Mn^{4+} ion density resulting into the strong zener double exchange mechanism between the Mn^{3+} and Mn^{4+} ions through O^{2-} [19].

vi. Large values of T_P for S2 and S3, well above RT, as well as T_P ~ 221K exhibited by 10% substitution of Sr^{2+} can be due to the compressive type nature of the strain at the interface of the films [21, 22].

In order to understand the magnetotransport behavior of the presently studied films, MR has been calculated using the formula:

$$MR(\%) = [(\rho_{H=H} - \rho_{H=0}) / \rho_{H=0}] \times 100$$

where, $\rho_{H=H}$ and $\rho_{H=0}$ are the resistivities under zero and applied field, respectively. Figure 4 shows the temperature dependent variation in MR for all the three films studied. It can be seen from figure 4 that, all the films exhibit maximum MR in the vicinity of their respective T_P. Maximum MR in the vicinity of T_P may be explained on the basis of field induced suppression of spin fluctuations and scattering of charge carriers. At T_P, there exists maximum magnetic disorder and magnetic field enhances the ferromagnetic spin ordering. S1 film exhibits MR ~ 25% at T_P while S2 and S3 films exhibit MR ~ 10 and 9%, respectively. Therefore, MR is found to decrease with increase in x that denotes the ferromagnetic phase is increase in the sample with Sr consternation which is responsible for the decrease in the magnetoresistance at T_P. 25% MR exhibited by S1 film is ascribed to the nanostructured granular morphology of the film having large non-magnetic grain boundaries, wherein the magnetic order can be improved by applying a small (~ 0.7T) magnetic field. All the films have large enough MR ~ T_P under relatively small applied field ~ 0.7T shows that all these nanostructured films have application potential in spintronic field.

Further, to explore the potential of presently studied nanostructured films for the practical applications, the temperature sensitivity of resistivity has been calculated using the formula [temperature coefficient of resistance (TCR)] –

$$TCR(\%/K) = [(1/R)(dR/dT)] \times 100$$

Figure 5 shows the variation in TCR, temperature sensitivity of resistivity, with temperature. All the films studied exhibit large sensitivity ~ 6 %/K while it is important to note that, S2 and S3 films exhibit maximum in TCR ~ 300K which useful for practical application in spintronic based devices operated at room temperature. The observed fluctuations in the temperature sensitivity in all the films can be attributed to the disordered interface of the films due to nanostructured morphology as well as low thickness of the films [23].

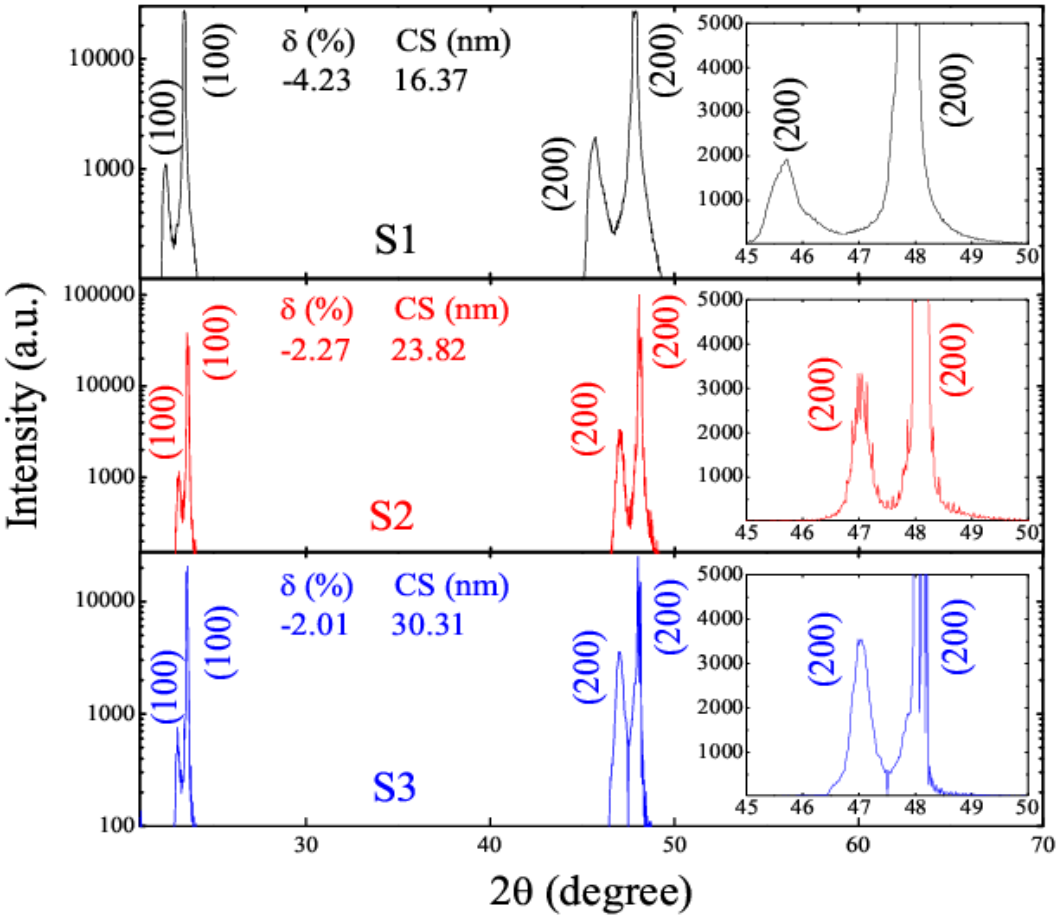

Figure 1: XRD patterns of nanostructured $La_{0.8-x}Pr_{0.2}Sr_xMnO_3$ manganite films Inset: Enlarged view of *(200)* XRD peaks and values of strain, δ, and crystallite size, CS, highlighted in the figure

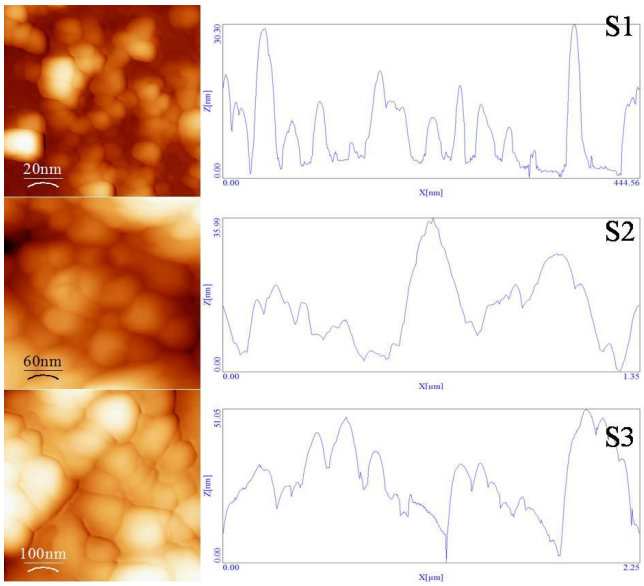

Figure 2: Left panel: AFM micrographs of nanostructured $La_{0.8-x}Pr_{0.2}Sr_xMnO_3$ manganite films Right panel: Granular height profile of nanostructured $La_{0.8-x}Pr_{0.2}Sr_xMnO_3$ manganite films

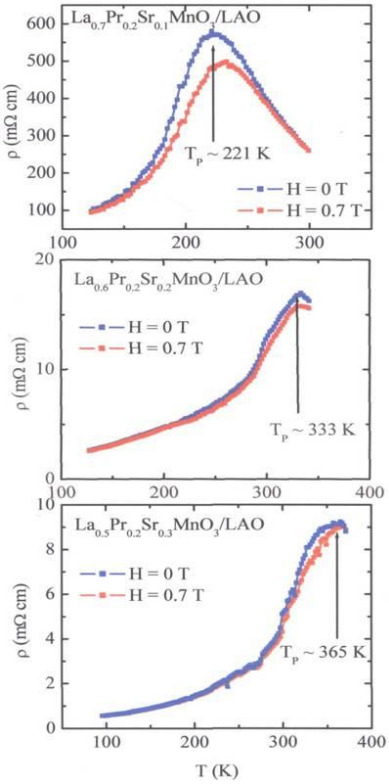

Figure 3: Variation in resistivity with temperature for nanostructured $La_{0.8-x}Pr_{0.2}Sr_xMnO_3$ manganite films under 0 and 0.7T fields

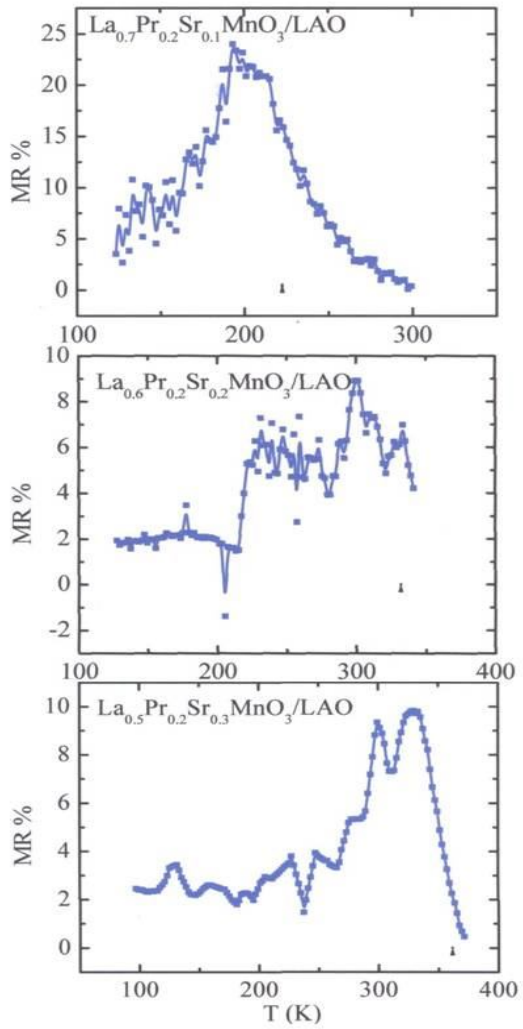

Figure 4: MR vs. T plots of nanostructured $La_{0.8-x}Pr_{0.2}Sr_xMnO_3$ manganite films under 0.7T field

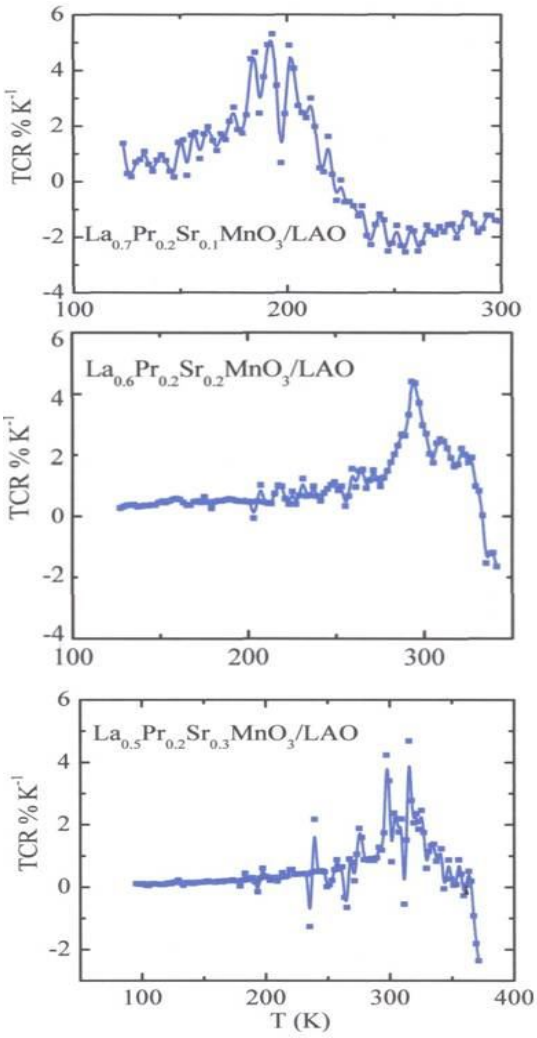

Figure 5: Variation in temperature sensitivity of resistivity [temperature coefficient of resistance (TCR)] of nanostructured $La_{0.8-x}Pr_{0.2}Sr_xMnO_3$ manganite films

Conclusions

In summary, nanostructured (50nm) films of $La_{0.8-x}Pr_{0.2}Sr_xMnO_3$ (LPSMO) (x = 0.1, 0.2 & 03) manganites have been successfully grown on $LaAlO_3$ (LAO) substrate using sol-gel and spin coating method. Structural and microstructural properties of the films show the improvement in crystallinity, structural strain, grain morphology and surface roughness with increasing substitution of Sr^{2+} in LPSMO manganite films. Structural and microstructural behavior dependent transport, magnetotransport and temperature sensitivity in LPSMO manganite system has been discussed in the light of tolerance factor, strain, crystallinity, grain size, grain boundary density and nature of the grain boundaries of the films.

Acknowledgements

Author is thankful to Government of Gujarat and Saurashtra University, Rajkot for providing financial support in the form of world class university grant for Nano Science Research.

Reference

[1] Ramirez, A.P., 1997, "Colossal Magnetoresistance", J. Phys.: Condens. Matter, 9(39), pp. 8171-8200

[2] Coey J.M.D., and Viret, M., 1999, "Mixed-Valence Manganites", Adv. Phys., 48(2), pp. 167-293

[3] Doggoto, E., Hotta T., and Moreo, A., 2001, "Colossal Magnetoresistant Materials: The Key Role of Phase Separation", Phys. Rep., 344(1-3), pp. 1-153

[4] Zener, C., 1951, "Interaction between the d-Shells in the Transition Metals. II. Ferromagnetic Compounds of Manganese with Perovskite Structure", Phys. Rev., 82(3), pp. 403-405

[5] Goodenough, J.B., 1998, "Jahn-Teller Phenomena in Solids", Annu. Rev. Nucl. Sci., 28, pp. 1-27

[6] Rathod, J.S., Khachar, Uma, Doshi, R.R., Solanki, P.S., and Kuberkar, D.G., 2012, "Structural, Transport and Magnetotransport in Nonmagnetic Al^{3+} Doped Mixed Valent $La_{0.7}Ca_{0.3}Mn_{1-x}Al_xO_3$ Manganites", Int. J. Mod. Phys. B 26(24), pp. 1250136:1-11

[7] Ravalia, Ashish, Vagadia, Megha, Trivedi, Priyanka, Keshvani, M.J., Khachar, Uma, Savalia, B.T., Solanki, P.S., Asokan, K., and Kuberkar, D.G., 2013, "Swift Heavy Ion Irradiation Studies on the Transport in $La_{0.8-x}Pr_{0.2}MnO_3$ Manganite Films", Adv. Mater. Res., 665, pp. 63-69

[8] Kansara, Sanjay, Pandya, D.D., Nimavat, Bhumika, Thaker, C.M., Solanki, P.S., Rayaprol, S., Gonal, M.R., Shah, N.A., and Kuberkar, D.G., 2013, "Structure-Transport Correlations in Mono-valent N^{+} Doped $La_{1-x}Na_xMnO_3$ Manganites", Adv. Mater. Res., 665, pp. 1-7

[9] Doshi, R.R., Solanki, P.S., Krishna, P.S.R., Das A., and Kuberkar, D.G., 2009, "Magnetic Phase Coexistence in Tb^{3+} – and Sr^{2+} – Doped $La_{0.7}Ca_{0.3}MnO_3$ Manganites: A Temperature – Dependent Neutron Diffraction Studies", J. Magn. Magn. Mater., 321(19), pp. 3285-3289

[10] Solanki, P.S., Doshi, R.R., Khachar, U.D., and Kuberkar, D.G., 2011, "Thickness and Microstructure Dependent Transport and MR in $La_{0.7}Pb_{0.3}MnO_3$ Manganite Films", Physics B, 406(8), pp. 1466-1470

[11] Vachhani, P.S., Markna, J.H., Kuberkar, D.G., Choudhary, R.J., and Phase, D.M., 2008, "High Field Sensitivity at Room Temperature in p-n Junction Based Bilayered Manganite Devices", Appl. Phys. Lett., 92(4), pp. 043506:1-3

[12] Markna, J.H., Vachhani, P.S., Kuberkar, D.G., Shah, N.A., Misra, P., Singh, B.N., Kukreja, L.M., and Rana, D.S., 2009, "Transport and Magnetotransport Studies on Sol–Gel Grown Nanostructured $La_{0.7}Pb_{0.3}MnO_3$ Manganites", J. Nanosci. Nanotechnol., 9(9), pp. 5687-5691

[13] Khachar, U.D., Solanki, P.S., Choudhary, R.J., Phase, D.M., Ganesan, V., and Kuberkar, D.G., 2012, "Room Temperature Positive Magnetoresistance and Field Effect Studies of Manganite Based Heterostructure", Appl. Phys. A, 108(3), pp. 733-738

[14] Parmar, R.N., Markna, J.H., Solanki, P.S., Doshi, R.R., Vachhani, P.S., and Kuberkar, D.G., 2008, "Grain Size Dependent Transport and Magnetoresistance Behavior of Chemical Solution Deposition Grown Nanostructured $La_{0.7}Sr_{0.3}MnO_3$ Manganite Films", J. Nanosci. Nanotechnol., 8(8), pp. 4146-4151

[15] Solanki, P.S., Doshi, R.R., Khachar, U.D., Vagadia, M.V., Ravalia, A.B., Kuberkar, D.G., and Shah, N.A., 2010, "Structural, Microstructural, Transport and Magnetotransport Properties of Nanostructured $La_{0.7}Sr_{0.3}MnO_3$ Manganites Synthesized by Coprecipitation", J. Mater. Res., 25(9), pp. 1799-1802

[16] Kuberkar, D.G., Doshi, R.R., Solanki, P.S., Khachar, Uma, Vagadia, Megha, Ravalia, Ashish, and Ganesan, V., 2012, "Grain morphology and size disorder effect on the transport and magnetotransport in Sol–Gel grown nanostructured manganites", Appl. Sur. Sci., 258(22), pp. 9041-9046

[17] Siwach, P.K., Goutam, U.K., Srivastava, P., Singh, H.K., Tiwari, R.S., and Srivastava, O.N., 2006, "Colossal magnetoresistance study in nanophasic $La_{0.7}Ca_{0.3}MnO_3$ manganite", J. Phys. D: Appl. Phys., 39(1), pp. 14-20

[18] Gaur, Anurag, and Varma, G.D., 2006, "Sintering Temperature Effect on Electrical Transport and Magnetoresistance of Nanophasic $La_{0.7}Sr_{0.3}MnO_3$", J. Phys.: Condens. Matter, 18(39), pp. 8837-8846

[19] Solanki, P.S., Doshi, R.R., Thaker, C.M., Pandya, Swati, Ganesan, V., and Kuberkar, D.G., 2009, "Transport and Magnetotransport Studies on Sol-Gel Grown $La_{0.7}Pb_{0.3}MnO_3$ Manganites", J. Nanosci. Nanotechnol., 9(9), pp. 5681-5686

[20] Solanki, P.S., Doshi, R.R., Khachar, U.D., Choudhary, R.J., and Kuberkar, D.G., 2011, "Thickness dependent transport and magnetotransport in CSD grown $La_{0.7}Pb_{0.3}MnO_3$ manganite films", Mater. Res. Bull., 46(8), pp. 1118-1123

[21] Chen, X.J., Habermeier, H.U., Zhang, H., Gu, G., Varela, M., Santamaria, J., and Almasan, C.C., 2005, "Metal-insulator transition above room temperature in maximum colossal magnetoresistance manganite thin films", Phys Rev. B, 72(10), pp. 104403:1-7

[22] Koo, T.Y., Park, S.H., Lee, K.B., and Jeong, Y.H., 1997, "Anisotropic Strains and Magnetoresistance of $La_{0.7}Ca_{0.3}MnO_3$", Appl. Phys. Lett., 71(7), pp. 977-979

[23] Khachar, Uma, Solanki, P.S., Choudhary, R.J., Phase, D.M., and Kuberkar, D.G., 2013, "Positive MR and Large Temperature-Field Sensitivity in Manganite Based Heterostructures", J. Mater. Sci. Technol., 29(10), pp. 989-994.